Beach safety: can drones provide a platform for sighting sharks?

Authors: Butcher, Paul A., Piddocke, Toby P., Colefax, Andrew P., Hoade, Brent, Peddemors, Victor M., et al.

Beach safety: can drones provide a platform for sighting sharks?

Paul A. Butcher [ID] [A,E], *Toby P. Piddocke*[A], *Andrew P. Colefax*[A], *Brent Hoade*[B],

Victor M. Peddemors [ID] [C], *Lauren Borg*[D] *and Brian R. Cullis*[D]

[A]NSW Department of Primary Industries, National Marine Science Centre, PO Box 4321, Coffs Harbour,
   NSW 2450, Australia.
[B]NSW Department of Primary Industries, Game licensing Unit, Port Macquarie, NSW 2444, Australia.
[C]NSW Department of Primary Industries, Sydney Institute of Marine Science, Mosman, NSW 2088,
   Australia.
[D]National Institute of Applied Statistics Research Australia, Faculty of Engineering and Information
   Sciences, University of Wollongong, Wollongong, NSW 2522, Australia.
[E]Corresponding author. Email: paul.butcher@dpi.nsw.gov.au

Abstract

Context. A series of unprovoked shark attacks on New South Wales (Australia) beaches between 2013 and 2015 triggered an investigation of new and emerging technologies for protecting bathers. Traditionally, bather protection has included several methods for shark capture, detection and/or deterrence but has often relied on environmentally damaging techniques. Heightened environmental awareness, including the important role of sharks in the marine ecosystem, demands new techniques for protection from shark attack. Recent advances in drone-related technologies have enabled the possibility of real-time shark detection and alerting.

Aim. To determine the reliability of drones to detect shark analogues in the water across a range of environmental conditions experienced on New South Wales beaches.

Methods. A standard multirotor drone (DJI Inspire 1) was used to detect shark analogues as a proxy during flights at 0900, 1200 and 1500 hours over a 3-week period. The 27 flights encompassed a range of environmental conditions, including wind speed (2–30.0 km h^{-1}), turbidity (0.4–6.4 m), cloud cover (0–100%), glare (0–100%), seas (0.4–1.4 m), swells (1.4–2.5 m) and sea state (Beaufort Scale 1–5 Bf).

Key results. Detection rates of the shark analogues over the 27 flights were significantly higher for the independent observer conducting post-flight video analysis (50%) than for the drone pilot (38%) (Wald $P = 0.04$). Water depth and turbidity significantly impaired detection of analogues (Wald $P = 0.04$). Specifically, at a set depth of 2 m below the water surface, very few analogues were seen by the observer or pilot when water turbidity reduced visibility to less than 1.5 m. Similarly, when water visibility was greater than 1.5 m, the detection rate was negatively related to water depth.

Conclusions. The present study demonstrates that drones can fly under most environmental conditions and would be a cost-effective bather protection tool for a range of user groups.

Implications. The most effective use of drones would occur during light winds and in shallow clear water. Although poor water visibility may restrict detection, sharks spend large amounts of time near the surface, therefore providing a practical tool for detection in most conditions.

Introduction

Unprovoked shark attacks (or shark bites) are dramatic events that command considerable public attention, and can increase tension between policy mandates for the protection of public safety and marine animal conservation (e.g. Neff 2012; Hazin and Afonso 2014; Gibbs and Warren 2015). In this context, unprovoked shark attacks are defined as those inflicted upon humans who have not attempted to deliberately interact with a shark (e.g. by feeding, touching, pursuing or capturing the animal), or those who are not otherwise engaged in activities

likely to attract sharks (e.g. spearfishing or cleaning fish) (West 2011; McPhee 2014; Ricci *et al.* 2016). The word 'attack' may not always accurately represent the motivations underpinning these interactions (Neff and Heuter 2013), but is used here for consistency. Both globally and in Australia, over half of all unprovoked attacks are attributed to white (*Carcharodon carcharias*), bull (*Carcharhinus leucas*) and tiger (*Galeocerdo cuvier*) sharks (West 2011; McPhee 2014). These three species are also implicated in almost all fatal attacks (West 2011; McPhee 2014).

Although shark attacks remain rare, the total number of global attacks increased 3-fold between 1982 and 2011 (McPhee 2014). Some of this increase reflects growing human population and greater overall participation in aquatic recreation (West 2011). The internet and widespread use of smartphones have also facilitated public awareness and reporting of shark attacks (West 2011). However, even after allowing for these factors, 30 years of data extracted from the Global Shark Attack File indicates that the proportional increase in attacks has outstripped population growth, suggesting a real, albeit small, increase (McPhee 2014). The mechanisms underpinning this rise are unclear, but may involve increased abundance of some prey species (especially marine mammals) (McPhee 2014; Chapman and McPhee 2016), changing human recreational behaviours (West 2011) and sharks' shifting habitat selection in marine ecosystems undergoing anthropogenic change (Hazin *et al.* 2008; Chapman and McPhee 2016). Greater shark abundance has also been raised as a possible cause, and although some local increases have been reported (e.g. Carlson *et al.* 2012; Froeschke *et al.* 2013), these appear insufficient to account for the global rise in attacks (West 2011; McPhee 2014). Regardless of the underlying causes, spatially and temporally clustered attacks, such as those along the coastlines of Recife (Hazin *et al.* 2008, 2013), Reunion Island (Blaison *et al.* 2015; Lemahieu *et al.* 2017), North and South Carolina (Amin *et al.* 2015) and off the Australian states of New South Wales (NSW; Neff 2012; Pepin-Neff and Wynter 2017) and Western Australia (WA; Gibbs and Warren 2015), usually result in public demands for risk mitigation (Hazin *et al.* 2008; Cliff and Dudley 2011; Hazin and Afonso 2014).

Shark attack clusters led to the establishment of the three longest-standing shark control programs globally: the NSW Shark Meshing Program (established 1937); the KwaZulu–Natal shark control program in South Africa (established 1952); and the Queensland Shark Control Program (established 1962) (Cliff and Dudley 2011). Initially, these programs focused solely on localised reduction of shark numbers using mesh nets and a system of large baited hooks suspended from surface floats, known as 'drum lines', to catch and kill sharks (Cliff and Dudley 2011; Reid *et al.* 2011; Sumpton *et al.* 2011). Gradually, increasing public concern over the programs' impacts upon both by-catch (typically non-target elasmobranchs, marine mammals and reptiles) and target species has seen governments searching for measures that improve protection for swimmers while minimising the impacts on sharks and other marine wildlife (Cliff and Dudley 2011; Hazin and Afonso 2014; Engelbrecht *et al.* 2017).

Some of the most recent alternative measures are based on modifications of existing technology. For example, the SMART (Shark Management Alert in Real Time) drumlines developed in Reunion Island incorporate satellite communications that automatically alert operators to a hooked animal via email, phone call and text message, enabling rapid release and/or relocation, usually after acoustic or satellite tagging (McPhee and Blount 2015). Other bather protection measures include: (1) physical barriers that aim to provide an impassable obstacle that separates sharks from people; (2) visual barriers, such as bubble curtains, that are not physically impassable but present aversive visual stimuli; and (3) barriers that aim to exploit sharks' aversion to particular electrical and electromagnetic stimuli (O'Connell *et al.* 2014*a*, 2014*b*, 2014*c*; McPhee and Blount 2015). Combined deterrents are also under investigation, such as the SharkSafe Barrier (Sharksafe Barrier™, Stellenbosch, South Africa; https://www.sharksafesolution.com/, accessed November 2019), which combines an electromagnetic deterrent with PVC piping that mimics dense kelp beds, creating a threshold that large sharks may be unwilling to cross (McPhee and Blount 2015; O'Connell *et al.* 2018). Personal deterrents, designed to be worn or carried by an individual swimmer or surfer, are not considered in detail here, but are reviewed by O'Connell *et al.* (2014*c*) and Hart and Collin (2015). Most of the above measures have reported some degree of success, but none represents a complete solution at either the individual or whole-of-beach scale. For example, physical barriers are susceptible to damage during rough seas (Cliff and Dudley 2011), and the species-specific nature of elasmobranch responses to electromagnetic stimuli may preclude universal application of electrical and electromagnetic deterrents (O'Connell *et al.* 2011, 2014*c*; Hart and Collin 2015).

The difficulty of identifying and implementing broadly applicable and cost-effective shark deterrents has given rise to measures aimed at shark detection (with subsequent warnings to swimmers) rather than deterrence. Detection approaches include trained observers working from elevated coastal vantage points (Engelbrecht *et al.* 2017), automated sonar systems (McPhee and Blount 2015; Parsons *et al.* 2015), acoustic tagging and monitoring programs (McAuley *et al.* 2016) and manned aerial patrols using fixed-wing aircraft or helicopters (McPhee and Blount 2015; Robbins *et al.* 2014).

Methodologically, aerial shark patrols represent a specialisation of the aerial surveys used to estimate wildlife distribution and abundance (e.g. Fleming and Tracey 2008; Rowat *et al.* 2009; O'Donoghue *et al.* 2010; Poole *et al.* 2013; Kleen and Breland 2014; Fuentes *et al.* 2015). Although aerial shark patrols aim simply to locate sharks and advise the public, rather than attempting formal estimates of abundance or distribution, high detection likelihoods and accuracy are important if the patrols are to effectively protect bathers (Robbins *et al.* 2014). Unfortunately, detecting sharks via aerial surveys can be difficult, because unlike air-breathing aquatic animals that spend a considerable portion of time at the water's surface, and therefore can be readily sighted from the air, white, bull and tiger sharks spend most of their time completely submerged (Holland *et al.* 1999; Dewar *et al.* 2004; Bonfil *et al.* 2005; Carlson *et al.* 2010). Aerial surveys have been used for locating sharks, particularly for species inhabiting shallow, clear water (Kessel *et al.* 2013), or when experimental designs allow flights to be undertaken only during periods of optimal visibility (Dicken and Booth

2013). However, these studies have not included formal estimates of detection likelihood, instead assuming that favourable conditions would facilitate detection of a high, but unspecified, proportion of the sharks present. Furthermore, manned aerial shark patrols are flown in a range of sea states and environmental conditions that may reduce detection rates by an unknown amount (Robbins *et al.* 2014). Studies quantifying detection likelihood in aerial shark patrols are scarce, but indicate low sighting rates. For example, Robbins *et al.* (2014) reported sighting rates of 12.5% and 17.1% for analogue sharks seen by observers from fixed-wing aircraft and helicopters, respectively. These rates suggest that, although aerial shark patrols may provide some psychological reassurance to bathers (Neff 2012), improved sighting rates and periods of surveillance 'cover' are required before they can be considered an effective bather protection measure (Robbins *et al.* 2014).

One option to improve the efficacy of aerial shark detection is to use drones, also known as remotely piloted aircraft systems (RPAS) or unmanned aerial vehicles (UAV), which are available in a variety of fixed-wing and multi-rotor configurations (Colefax *et al.* 2018). Drones increasingly present an alternative to manned aircraft for a variety of wildlife survey and detection tasks (Kudo *et al.* 2012; Martin *et al.* 2012; Linchant *et al.* 2015; Evans *et al.* 2015; Kiszka *et al.* 2016; Colefax *et al.* 2019; Kelaher *et al.* 2019). In the context of shark patrols, drones offer several potential advantages over manned aircraft because they can operate at individual beaches, and fly constantly at lower airspeeds and altitudes than are physically or legally possible for manned aircraft (Kudo *et al.* 2012; Robbins *et al.* 2014, but see Linchant *et al.* (2015) for possible exceptions). Drones can also carry polarising filters to facilitate viewing in real time, or hyperspectral sensors for digitally enhancing images for post processing so that we can 'see' further below the water's surface than human observers in manned aircraft (Stein *et al.* 1999; Schoonmaker *et al.* 2011). Furthermore, drones are more cost-effective to operate than manned aircraft for small-scale surveys, produce fewer environmental impacts and pose a lower risk to both operators and bystanders (Kudo *et al.* 2012; Martin *et al.* 2012; Linchant *et al.* 2015).

Although recent technological advances have seen drones used in many wildlife survey applications, their capacity to detect predatory sharks remains untested. The primary aim of the present study is to quantify the effectiveness of detecting submerged shark analogues using drones across a range of environmental conditions representative of those likely to be encountered along the eastern Australian coastline. Beyond the realm of bather protection, the research also aims to determine the utility of drones as a shark survey method.

Materials and methods

Study site

The experiment was completed at Hills and Korora Beach (30°15.093′S, 153°8.593′E), Coffs Harbour, New South Wales, Australia during November and December 2015, using a drone and two-dimensional shark analogues. The flight path covered a 1.9-km length (0.950 m either side of the control station) of nearshore sand and rocky-reef habitat, creating a 3.8-km circuit ~35 m from the backline of the surf break on any given day.

Aircraft configuration and operation

All flights were completed using a DJI Inspire 1 (DJI, Shenzhen, China) quadcopter drone with a DJI Zenmuse X5 camera (DJI MFT 15 mm F/1.7 ASPH lens) and vibration absorbing board, and a circular polarising filter (ProMaster Digital HGX CPL – 46 mm). The camera was set to record the entirety of each flight in 4K video (3840 × 2160 pixels), and the pilot took still images (16-megapixel resolution) when an animal was sighted. The drone was flown at a height of 60 m to provide an uninterrupted 70-m wide swathe, with the camera pitched at 10 degrees forward of nadir to optimise navigation and observation (irrespective of sun position). The drone was controlled by a multi-functional remote utilising 2.4 GHz wireless communication. Flights were maintained within line-of-sight by the drone's pilot, in accordance with Australia's Civil Aviation Safety Authority (CASA) regulations. The drone's camera feed was viewed in real time by the pilot, using a 24.6-cm Apple iPad Air (Cupertino, CA, USA) screen with a protective hood on the top and sides to minimise sun glare. All flights were completed using one battery with up to 20% remaining.

Shark analogues

For the experiment, two-dimensional shark analogues were used within the survey area (following the procedures of Robbins *et al.* 2014). Although the use of live sharks would be preferred, the use of analogue or decoy animals is well established in the aerial survey literature as an effective means of rigorously testing detection efficiency, because the number and positioning of analogues is known to researchers, but not to the observers or pilot (e.g. Jones *et al.* 2006; Koski *et al.* 2009; Robbins *et al.* 2014). Each analogue in the experiment measured 2430 mm (total length) by 1190 mm (pectoral fin width), and was constructed of 11-mm marine plywood. Both sides of the analogues were painted grey to replicate large oceanic sharks (Robbins *et al.* 2014), with two shaped as white sharks and two as hammerhead sharks (*Sphyrna* sp.) (Fig. 1).

One to four analogues were deployed from a vessel at a given location 2 m below the surface in 2.0–6.3 m water depth. This depth was chosen because poor detection rates have previously been reported for shark analogues positioned more than 2.6 m deep (Robbins *et al.* 2014). The actual water depth is important because the change in colour or background may influence the ability to locate an analogue. To enable horizontal orientation in the water, each analogue was attached at four points on the underside using wire cables terminating at a single metal ring attached to a rope and anchor. For retrieval purposes, a 50-mm float (not visible to the pilot) was attached to the analogue's upper surface with clear monofilament line. All analogues were positioned within 70 m of the back line of the surf break to ensure they were visible within the strip width of the drone camera.

Environmental data

At each prescribed flight time, the pilot recorded 15 environmental variables, including: average and maximum wind speed (km h^{-1}) and direction (as a bearing); barometric pressure (hPa); air temperature (°C); rainfall over the preceding 24 h (mm); sea and swell height (average and maximum; m); and direction (as a bearing) and humidity (%) from a meteorological station nearby
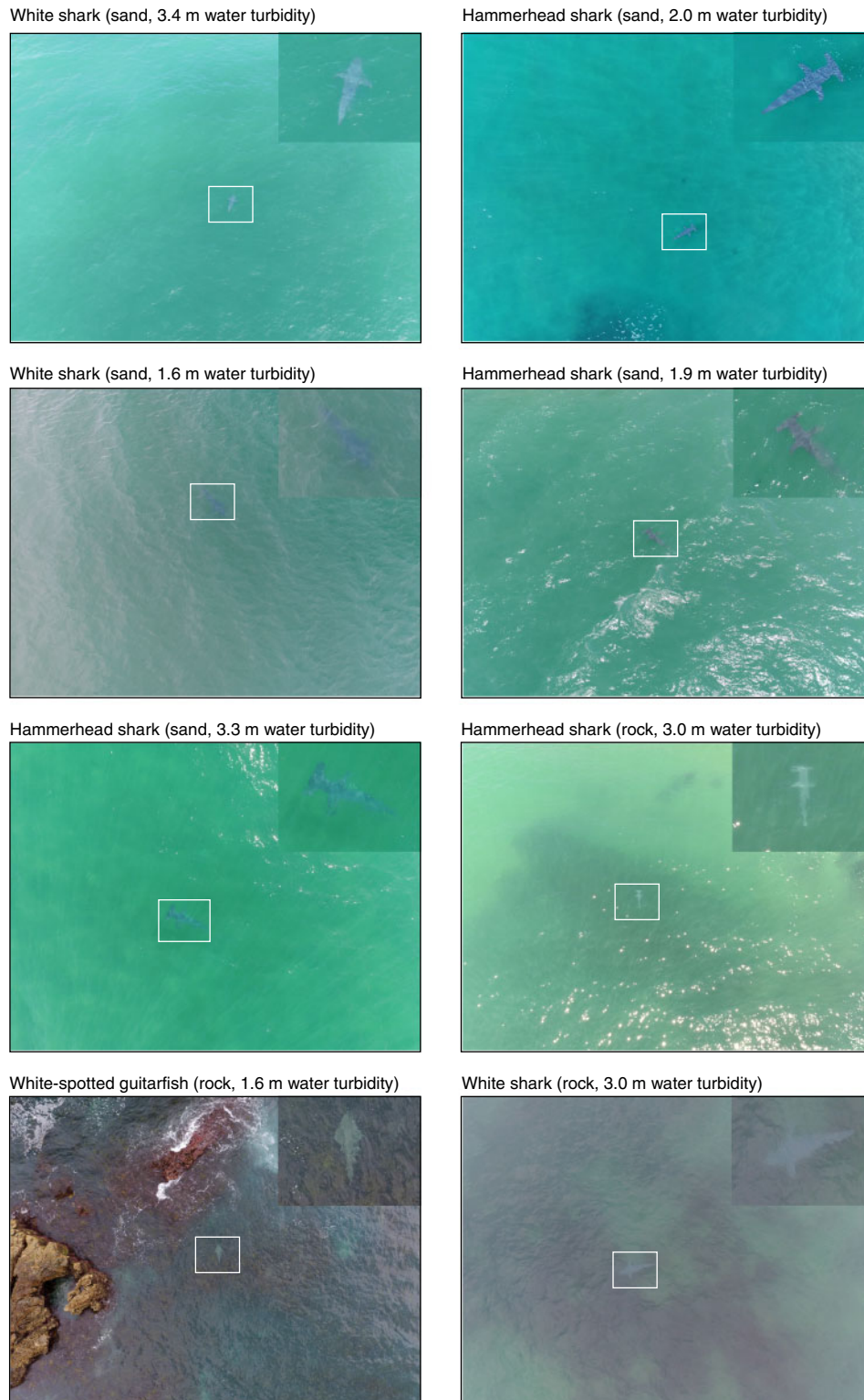
Fig. 1. Images of hammerhead shark and white shark analogues across different water turbidity (m) and substrates (sand and rock) in comparison with a live white-spotted guitarfish (*Rhynchobatus australiae*) seen during the trials. White square indicates the location of the analogue.

(Manly Hydraulics Laboratory and Bureau of Meteorology). Sea state (Beaufort scale 0–5 Bf) and cloud cover (scored as a scale from 0 for no cloud to 8 for complete cloud cover) were determined by personal observation, and water turbidity (m) or water visibility at each shark analogue was measured with a Secchi disk (m) by the boat crew before each flight. When taking measurements, if the water visibility exceeded the water depth (i.e. the seabed was visible), then the visibility was instead measured at a nearby location to the deployed analogue at a greater depth. At the end of the flight, the percentage of battery remaining was recorded, as were survey and flight end times.

All recorded environmental variables were included in the analysis except for rainfall, swell height and direction (average and maximum) and maximum wind speed. The rainfall variable showed 90% of observations as 0 mm rainfall, and the remaining 10% were recorded as only 0.1 mm. Similarly, there was insufficient variation in the swell average variable, ranging from 0.82 to 1, with 80% of observations taking a single value of 1. Observations for the maximum swell variable ranged from 1.4 to 2.1, which was insufficient variation to detect any effects. Average wind speed and maximum wind speed had a near one-to-one relationship, so only average wind speed was included in the model.

For statistical analysis, the wind speed variable ($km h^{-1}$) had four categories: calm (0–5 $km h^{-1}$); light (6–10 $km h^{-1}$); moderate (11–15 $km h^{-1}$); and strong (>16 $km h^{-1}$). The wind direction variable, which originally had seven categories (east, north, north east, north west, south, south east and south west), was re-categorised to four (south–south west, east–south east, north–north east and west–north west) as prevailing wind directions. The air temperature (°C) and humidity (%) variables were rounded to the nearest whole numbers, and the barometric pressure variable (hPa) was rounded to one decimal place.

Flights

Twenty-seven flights were completed over 3 weeks and up to 3 days per week, with flights occurring at 0900, 1200 and 1500 hours on each flying day. The same commercial pilot operated the drone throughout the experiment, with the pilot deciding whether flights were to proceed based on environmental conditions.

A GPS reference point was positioned at the northern, middle and southern ends of the circuit so that all flights paths were consistent with the northern and southern boundaries. The ground control station (GCS) from which the drone would take off and land was positioned on the beach adjacent to the midpoint of the flight path. For each flight, the drone was flown manually at 40 $km h^{-1}$ parallel to the beach in a northerly direction to the northern extremity of the flight path (0.95 km), before turning 180° and travelling south (1.90 km) to the southern extremity. The drone then turned around (180°) and returned along the same flight path (0.95 km) to the flight circuit's midpoint, before landing at the GCS. The entirety of each flight was recorded, with additional photographs of any sighted shark analogues. Any analogue sightings made by the pilot were also communicated verbally to an observer standing next to the pilot, who recorded the time, location, analogue shape and flight direction.

Drone footage review

In the week following the flights, all flight videos were reviewed at real-time pace by a single observer in a laboratory. For independence, this was done without the observer knowing the date, day or flight number. The observer independently recorded all analogues visible in the footage, and the drone's direction of travel at the time each analogue was detected. For each sighting, the laboratory-based observer also recorded a value for glare (0–4) based on the percentage of affected screen. A mean glare value for each flight was calculated, and a per-flight glare category (0, nil; 4, extreme) assigned. All footage was observed using a PC (Dell Optiplex 9020) with a 58.4-cm (1920 × 1080 resolution) display. The main observer and a second observer completed further assessments of random flights for compatibility, but these were not included in the overall analysis because they were the same.

Statistical analysis

The analysis accounted for the structure of the experimental design when examining the influence of environmental factors on sighting rates. The model used in the analysis accommodated for the dependence in the response variable through unmitigated, shared covariates; this reduces the likelihood of false associations caused by confounding environmental variables with plot factors. For the formation of the model, we used the approach of Smith and Cullis (2019), thereby defining the plot and treatment factors, their associated structure and the design function for the randomisation of treatments. This provided the terms, which were included in the generalised linear mixed model (GLMM), as well as determining the status (fixed or random) of all terms in the model. Observations for analogue sightings are not independent because their deployment remained the same for both flight directions (north and south); thus, we used a GLMM with random terms to allow for dependence between observations. A logistic GLMM with a logit link was fitted to the binary response of detectability, coded as 0 (for non-detection) and 1 (for detection). The pilot and laboratory observer data were analysed together, as is typical with double-observer data in the field of ecology (e.g. Bernard *et al.* 2013; Strobel and Butler 2014).

The experiment can be considered a multi-phase experiment, where Phase I involved the construction of the shark analogues, with two analogues for each species, and Phase II was the deployment of analogues. The plot factor for Phase I was the shark 'analogue' (four levels), and the treatment factor was 'species' (two levels). The treatment structure was 1 + species, where 1 represents the overall mean, and the plot structure was 'analogue'. For Phase II, the set of plot factors were 'Flight' (two levels), 'Week' (three levels), 'Day' (three levels), 'Time' (three levels), 'Viewing' (two levels) and 'Location' (four levels). We further defined an additional plot factor 'Set', which was a factor for levels that were the unique combinations of the three plot factors 'Week', 'Day' and 'Time'. For each level of 'Set', analogues were deployed to each of the randomly chosen locations within the pre-determined grid. The number of analogues that were deployed varied from zero to four. This approach was adopted to mask the true number of analogues deployed for any given set from the pilot and the observer. There were three

sets that had no analogues deployed. These sets were discarded from the analysis of detectability for analogues, but used in the overall data. The factor 'Viewing', with two levels, corresponds to the two viewings of the footage at each deployment by the pilot and then subsequently by the laboratory observer. Finally, 'Flight' has two levels, north and south, corresponding to the flight direction. The plot structure is given by:

$$Flight + Week + Week : Day +$$
$$Week : Day : Time + Week : Day : Time : Location +$$
$$Week : Day : Time : Location : Viewing +$$
$$Flight : Week + Flight : Week : Day + Flight : Week : Day : Time +$$
$$Flight : Week : Day : Time : Location +$$
$$Flight : Week : Day : Time : Location : Viewing$$

where *Flight* : *Week* : *Day* : *Time* : *Location* : *Viewing* indexes the observational units.

These treatment and plot structures lead to what is termed the working GLMM, where all model terms in the plot structure are assumed to be random terms. Terms in the treatment structure were then fitted as fixed terms, except for those terms in the plot structure of Phase I (i.e. Analogue), which were fitted as random.

$$fixed = \sim 1 + Species + Observer + Species : Observer$$
$$random = \sim Analogue + Flight + Week + Week : Day +$$
$$Week : Day : Time + Week : Day : Time : Location +$$
$$Week : Day : Time : Location : Viewing +$$
$$Flight : Week + Flight : Week : Day + Flight : Week : Day : Time +$$
$$Flight : Week : Day : Time : Location +$$
$$Flight : Week : Day : Time : Location : Viewing$$

The working GLMM was then extended to the full set of environmental factors and variates (Table 1). To assist with the notation, we refer to '*X*' as the matrix of covariates and dummy factors associated with the environmental factors and variates listed in Table 1. The GLMM was extended by including *X*, as well as the interaction of species and observer with *X*. Terms were then removed from this full GLMM using backward elimination, with respect to marginality. That is, all interaction terms were considered before examination of the main effects of *X*.

All analyses were conducted in the R (R Development Core Team 2015) package ASReml-R, which fits GLMMs using the approach of Breslow and Clayton (1993). Inference for fixed effects was conducted using approximate Wald-type pivots (Butler *et al.* 2009).

Results

Twenty-seven flights (mean ± s.d., 12:50 ± 1:55 min : seconds) across 9 days were completed over 3 weeks. The 54 shark analogues (23 hammerhead and 31 white sharks) were set in water depths between 2.0 and 6.3 m (mean ± s.d., 3.6 ± 1.1 m), over sand (39 deployments) and reef (15 deployments) habitats. Only one flight at 0900 hours was delayed due to rain, while the rest went as scheduled across the variety (mean ± s.d., range) of environmental conditions: wind speed (14.6 ± 7.5 km h^{-1},

Table 1.   Summary of environmental factors and variates considered in the generalised linear mixed model for detecting shark analogues
Where cells in the Factor column are False, range is provided, where they are True, levels are provided

Variable	Factor	Range (min–max) or levels
Air temperature	False	23.5–28.4°C
Barometric pressure	False	1010–1021 hPa
Cloud cover	True	0, 1, 2, 3, 6, 7, 8
Glare	True	0, 1, 2, 3
Habitat	True	reef and sand
Humidity	False	52–80%
Sea state	True	1, 2, 3, 4
Water turbidity	False	0.4–6.3 m
Water depth	False	2.0–6.3 m
Wind direction	True	ESE, NNE, SSW, WNW
Wind speed	True	Calm, light, moderate, strong

2.0–30.0 km h^{-1}); turbidity (2.1 ± 1.1 m, 0.4–6.4 m); humidity (67.1 ± 6.8%, 52–80.0%); barometric pressure (1014 ± 3.3 hPa, 1008–1021 hPa); cloud cover (3.7 ± 3.1, 0–8); air temperatures (surface: 25.5 ± 1.2°C, 23.5–28.4°C); glare (1.2 ± 0.7, 0.0–3.0); seas (0.7 ± 0.3 m, 0.4–1.4 m); swells (1.8 ± 0.2 m, 1.4–2.5 m); and sea state (2.3 ± 1.2 Bf, 1.0–5.0 Bf).

Because a given analogue had two chances of being detected (north- and south-bound flight segments), there was a total of 108 possible analogue detections, of which 67 were not sighted by either the pilot or observer. In total, 31 analogues (29%) were sighted by both the pilot and laboratory observer, and an additional 10 analogues (9%) were detected by the laboratory observer but not the pilot. No analogues were detected by the pilot and not the observer. Fig. 2 presents a jittered scatter plot of the analogues detected and missed by the pilot and laboratory observer against water turbidity (m), which indicates that the detection probability is very low in conditions where the water visibility is less than 1.5 m. Specifically, of the 31 analogue sightings detected by both the pilot and observer, only two of the sightings for each group occurred when the water visibility was less than 1.5 m (Fig. 2). Deployments when the water visibility was less than 1.5 m provide no insight into additional factors that may affect detection. The remaining analyses were therefore conducted on those deployments for which water visibility was greater than 1.5 m ($n = 78$). Of these 78 shark analogue deployments in water visibility >1.5 m, 29 (38%) were detected by the pilot and 39 (50%) from post analysis by the observer. There were no false positives observed where either the pilot or laboratory observer recorded a shark analogue when there were none deployed.

Detectability

For the GLMMs exploring the influence of environmental variables relating to probability of analogue detection by the pilot or laboratory-based observer, all treatment terms were non-significant and dropped from the final model except for the main effect of water depth (Table 2). The term 'species' was retained because of the treatment structure, although there was no significant difference ($P = 0.50$) in detection probability between hammerhead (0.34 ± 0.64) and white shark (0.47 ± 0.64) analogues (Table 2).
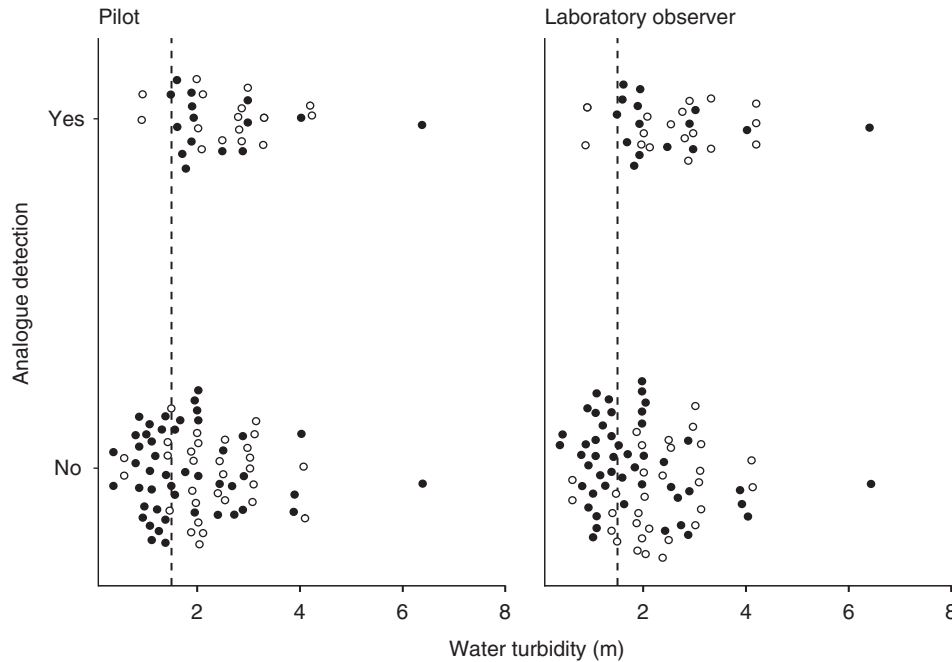
Fig. 2. Scatter plot of jittered shark-sighting rates from the pilot and laboratory observer (hollow circle, hammerhead shark analogue; black circle, white shark analogue) against water turbidity (m). Dashed line shows the 1.5 m-turbidity level and analogues that were excluded from the formal analysis of detection probability.

Table 2. Summary of conditional Wald test statistical model for detection probability, and associated probabilities of significance, based on an asymptotic Chi-squared reference distribution

d.f., degrees of freedom; F.con, *F*-statistic; pchisq, cumulative Chi-squared reference distribution

Pilot	d.f.	F.con	pchisq
(Intercept)	1	2.263	0.133
Species	1	0.457	0.499
Observer	1	4.446	**0.035**
Water depth	1	4.184	**0.040**

There was a significant difference ($P = 0.04$; Table 2) in detection probability between the pilot (0.30 ± 0.61) and the laboratory observer (0.51 ± 0.61), with a log odds ratio of 0.916. The odds of detecting an analogue were 2.5 times greater for the laboratory observer than for the pilot. Water depth was also significant ($P = 0.04$), with a log odds ratio of -0.874. Specifically, an increase in water depth by 1 m results in a 58% reduction in the odds of detection. The predicted detection drops below 50% when the water depth exceeds 3.5 m (Fig. 3). However, there were three detections by both the pilot and observer in water depth >5 m and on both flight directions. These detections involved the same white shark analogue, and occurred over a sandy substrate on a windless day with smooth sea conditions.

The estimates on the logit scale for the between-flight (Week : Day : Time : Location) and within-flight variance (Flight : Week : Day : Time : Location) were 0.65 and 3.38, respectively. An approximate measure of dependence between flights (0.84) was given by the within-flight variance divided by the sum of the within- and between-flight variance. There was considerable
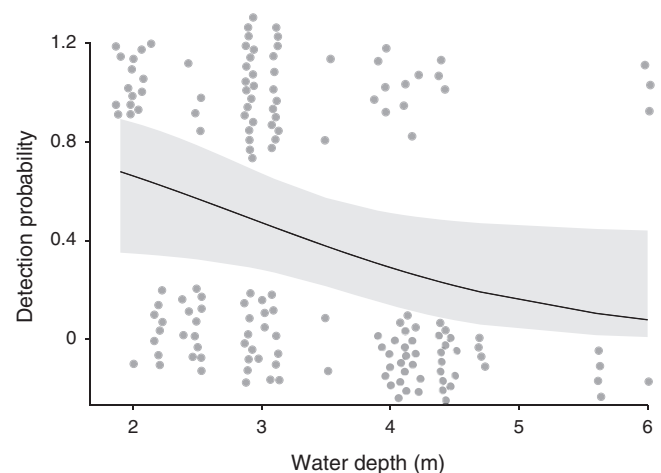

Fig. 3. The jittered binary outcomes (top, seen; bottom, not seen) with the approximate 95% pointwise coverage interval for the predicted probability for detection (shaded area) for shark sighting rates against water depth (m) when water turbidity was >1.5 m depth.

correlation in detection probabilities between flight directions, which was expected given that the location of analogue deployments remained the same for flights within a set. However, the random component of the GLMM fitted accounted for this dependence.

Discussion

The present study has quantified the diverse range of coastal conditions under which drones can operate, demonstrating their utility for detecting objects in the water (in this case shark analogues), particularly in conditions of reasonable water visibility and depth. Depending on the environmental conditions, drones can potentially be used to spot sharks or other marine fauna along coastal beaches, and could supplement existing aerial survey methods (Colefax *et al.* 2019). Furthermore, drones would provide a cheaper and more versatile platform than manned aircraft for beach authorities and various user groups for localised coastal areas (Colefax *et al.* 2018). The potential benefits that drones can offer for bather protection, and specifically shark attack mitigation, are discussed by considering the underlying mechanisms that may affect their use.

Water turbidity, which was high throughout the study, had a strong negative relationship with detection probability. Specifically, when the depth of sightability (governed by turbidity) was shallower (<1.5 m) than the depth of the shark analogues (2 m), detection probability was very low, with neither the pilot nor laboratory observer able to identify the shark analogues. Turbidity is recognised as a major factor affecting data reliability in aerial surveys because it decreases the depth in the water column at which an animal can be sighted, thereby decreasing detection probability proportionately to dive behaviour (Pollock *et al.* 2006; Hodgson *et al.* 2013; Hagihara *et al.* 2014; Fuentes *et al.* 2015). In clear water, the pilot and observer detected analogues, but detection probability across the survey was skewed because water clarity was poor for much of the study.

Water depth had a significant effect on detection probability, particularly at depths >3.5 m. This is likely because light attenuation changes with water depth, altering contrast between the grey shark analogue and the substrate. Similarly, sighting rates for dugong (*Dugong dugon*) decreased with water depth and turbidity (Pollock *et al.* 2006; Hodgson *et al.* 2013). In deeper water, wavelengths of light are either scattered or absorbed before reflecting off the substrate, creating a darker ocean colour and masking the grey shark-like colour of the analogues (Bloom *et al.* 2019). Conversely, in shallower water, where the depth of sightability is greater than the water depth, light is reflected from the sand or reef substrate, giving the water a lighter appearance and allowing better contrast with the silhouette. Depth-related differences in light attenuation and reflection suggest that multispectral and hyperspectral sensors might allow better image contrasting through frequency band selection (Colefax *et al.* 2018).

Although glare (as sea surface reflectance) did not significantly affect sighting rates (through perception biasing; Pollock *et al.* 2006), glare effects were detectable, particularly around midday and at times when sea surface conditions produced wavelets. The effects of sea surface reflectance can typically be reduced in manned aerial surveys by polarisation (Zhang *et al.*

2017), such as having observers wear polarised sunglasses (Alves *et al.* 2013). In drone-based aerial surveys, the equivalent is achieved by applying appropriate circular polarising filters for the light intensity at a given location, as was done in this experiment. Further measures can also be taken to potentially reduce sea surface reflection, such as altering the drone's orientation and making minor adjustments to the gimbal angle with regard to the sun's position, particularly when near its zenith (Zhang *et al.* 2017). However, these measures may have consequences for the consistency of flight parameters (e.g. transect width), and perhaps depth of sightability due to altered sensor viewing angles.

The present study did not identify significant effects of wind and sea state on sighting rates. This counterintuitive result may be an artefact, reflecting the model's inability to distinguish wind and sea-state effects from the high turbidity levels present throughout much of the study. Alternatively, strong winds and rough seas may actually impair marine fauna sighting rates less for drones than for manned aircraft, because drones are flying substantially slower and lower. Although other drone-based marine surveys have indicated likely declines in detection probability associated with increasing sea states (Koski *et al.* 2009; Hodgson *et al.* 2013), it is likely that the comparatively lower altitudes, smaller search area and slower speeds of drone-based surveys would allow longer scanning time over an area for the observer and pilot, and buffer some of the adverse effects on detection rates in comparison to manned aircraft (Colefax *et al.* 2018). To conclusively determine if detection probability from drone-based shark surveillance is less affected by environmental variables, including wind and sea state, an empirical investigation directly comparing it with manned aircraft is required.

Flights throughout the study were exposed to a range of environmental conditions, including fresh wind strengths of 30 km h^{-1} and sea states up to 5 Bf. Manned aircraft can also conduct aerial shark surveillance during these conditions, but generally avoid doing so because sighting probability is significantly impaired (Rowat *et al.* 2009; Robbins *et al.* 2014). Manned aerial surveys are costly ($\sim$AU\$1200 per hour), and the reduced sighting probabilities characteristic of high winds and rough seas often result in decisions to restrict operations to sea states less than 3 Bf and winds (<30 km h^{-1}) (Rowat *et al.* 2009; Kleen and Breland 2014; Fuentes *et al.* 2015). However, the array of real-time tracking buoys that detect dangerous sharks along 21 coastal beaches in NSW has shown that they are present across all environmental conditions (Paul Butcher, NSW DPI, unpubl. data).

The small but significant difference in sighting rates between the pilot and the observer indicates a degree of perception biasing in field-based analogue detections. Pilot perception error was noticeable between water depths of 3.5 and 4.5 m, where the observer detected more shark analogues than the pilot did. These differences in sighting rates usually manifested in conditions of low (but still >1.5 m) water clarity and over deeper water, so the shark analogues had only very faint background contrasting for the pilot to detect in real time. The results from the present study suggest that in shallower or clearer conditions, there would likely be negligible difference in detection probability between the pilot and observer. In scenarios where detection becomes increasingly difficult, perception biases in field detections may

be explained by: (1) attention of the pilot spread across multiple tasks; (2) sun glare on the telemetry screen; (3) the telemetry screen size and/or decreased resolution compared with post-processing; or (4) the observer's ability to pause, slow down or replay transect segments for sighting determinations.

Australian civil aviation regulations stipulate that drones must remain within the pilot's line-of-sight (unless under special exemption), and that the drone's condition and surrounding airspace must be monitored for hazards and air traffic throughout the flight. The multi-tasking nature of conducting these tasks while observing the video feed may have reduced the pilot's detection performance (Adler and Benbunan-Fich 2012). One or two observers might significantly increase the probability of detecting objects on the screen. Additionally, although shading was used on the top and sides of the telemetry screen to reduce sun glare and enable a clearer picture, viewing drone footage on a larger, higher resolution screen in a controlled environment would likely facilitate object detection. Measures including the use of high resolution 'first-person-view' goggles (such as DJI goggles), a large protected screen showing the live telemetry to an observer, or a brighter screen (i.e. CrystalSky Ultra, DJI, China) could improve real-time object detection by drone pilots in the field. Alternatively, advancements in automatic software recognition may assist the pilot in identifying otherwise missed detections. Computer-based object recognition is a research focus in this field – and will inevitably lead to increased post-processing efficiency of drone-captured imagery – but is still largely in developmental stages, particularly in heterogeneous environments (Chabot and Francis 2016; Seymour *et al.* 2017; Gu *et al.* 2018; Saqib *et al.* 2018).

Despite all scheduled drone flights proceeding throughout the 3-week survey period, the presence of rain did delay one flight as the drone used in this study, like most drones, was not rated to fly in wet conditions. Although water-resistant drones exist, they generally have much shorter ranges and achieve shorter flight durations than equivalent non-water-resistant variants (Fiori *et al.* 2017). Marine fauna surveys from manned aircraft technically can operate during rain, but avoid doing so because it impairs the sightability of marine fauna (Pollock *et al.* 2006; Rowat *et al.* 2009; Kleen and Breland 2014). Similarly, rainy conditions would likely impair faunal sightability even if water-resistant drones were used. Precipitation is therefore potentially the main limitation on drone-based shark surveillance, because it can either force surveillance operations to cease or impede faunal sightings (Colefax *et al.* 2019).

The use of shark analogues to determine sighting rates in the present study provides an indication of performance, but, for a given shark size and water depth, a moving shark would undoubtedly be detected more easily than a still replica. The difference in detection probability between a shark analogue and live shark was assumed (but not tested) to be negligible from manned aircraft (Robbins *et al.* 2014). However, due to their low speed and narrow strip width, drones survey areas more intensively, resulting in a shark being captured within the sensor for a longer period (often >5 s). Movement may therefore be more important as a distinguishing factor for faunal detection using aerial surveys than previously assumed, particularly for surveys using drones.

The applicability of drones for aerial shark surveillance will depend partly on location- and jurisdiction-specific surveillance requirements. Demand is growing for reliable shark attack mitigation with minimal impact on marine animals (Cliff and Dudley 2011; Hazin and Afonso 2014; Meeuwig and Ferreira 2014).

Conclusions

Our results suggest that drones are a potential platform for non-invasive shark surveillance, and that further research into refining operational procedures and incorporating new technologies will allow for improvements in detection reliability across a broader range of operating conditions. In time, drones may offer better detection reliability than manned aircraft, with developments in real-time object recognition software likely to further improve detection probabilities. Although adverse environmental conditions impacted sighting rates, these conditions also likely correspond with few-to-no water users, arguably reducing the need for shark surveillance (de Freitas 2015). An empirical investigation to determine the effects of weather variables on the presence of water users could, in future, better define the environmental conditions under which reliable sighting rates are imperative. Under the range of environmental conditions seen during the present study, shark detection will be optimised: when the water turbidity state allows vision to a depth of at least 1.5 m; in shallow water depths (<3.5 m); and when a dedicated observer, rather than the drone pilot, is responsible for shark detection. This study has shown that drones can offer an alternative shark detection tool that could meet increasing demands for bather protection while minimising harm to marine life.

Conflicts of interest

The authors declare no conflicts of interest.

Acknowledgements

References

Adler, R. F., and Benbunan-Fich, R. (2012). Juggling on a high wire: multitasking effects on performance. *International Journal of Human–Computer Studies* **70**, 156–168. doi:10.1016/J.IJHCS.2011.10.003

Alves, M. D. O., Schwamborn, R., Borges, J. C. G., Marmontel, M., Costa, A. F., Schettini, C. A. F., and Araújo, M. E. (2013). Aerial survey of manatees, dolphins and sea turtles off northeastern Brazil: correlations with coastal features and human activities. *Biological Conservation* **161**, 91–100. doi:10.1016/J.BIOCON.2013.02.015

Amin, R., Ritter, E., and Wetzel, A. (2015). An estimation of shark-attack risk for the North and South Carolina coastline. *Journal of Coastal Research* **315**, 1253–1259. doi:10.2112/JCOASTRES-D-14-00027.1

Bernard, A., Gotz, A., Kerwath, S., and Wilke, C. (2013). Observer bias and detection probability in underwater visual census of fish assemblages

measured with independent double-observers. *Journal of Experimental Marine Biology and Ecology* **443**, 75–84. doi:10.1016/J.JEMBE.2013.02.039

Blaison, A., Jaquemet, S., Guyomard, D., Vangrevelynghe, G., Gazzo, T., Cliff, G., Cotel, P., and Soria, M. (2015). Seasonal variability of bull and tiger shark presence on the west coast of Reunion Island, western Indian Ocean. *African Journal of Marine Science* **37**, 199–208. doi:10.2989/1814232X.2015.1050453

Bloom, D., Butcher, P. A., Colefax, A. P., Provost, E. J., Cullis, B. R., and Kelaher, B. P. (2019). Drones detect illegal and derelict crab traps in a shallow water estuary. *Fisheries Management and Ecology*. doi:10.1111/FME.12350

Bonfil, R., Meÿer, M., Scholl, M. C., Johnson, R., O'Brien, S., Oosthuizen, H., Swanson, S., Kotze, D., and Paterson, M. (2005). Transoceanic migration, spatial dynamics, and population linkages of white sharks. *Science* **310**, 100–103. doi:10.1126/SCIENCE.1114898

Breslow, N. E., and Clayton, D. G. (1993). Approximate inference in generalised linear mixed models. *Journal of the American Statistical Association* **88**, 9–25. doi:10.1080/01621459.1993.10594284

Butler, D., Cullis, B. R., Gilmour, A., Gogel, B. and Thompson, R. (2009). ASReml-R reference manual. Release 4 edition. Technical report. (VSN International: Hemel Hempstead, UK.)

Carlson, J. K., Ribera, M. M., Conrath, C. L., Heupel, M. R., and Burgess, G. H. (2010). Habitat use and movement patterns of bull sharks *Carcharhinus leucas* determined using pop-up satellite archival tags. *Journal of Fish Biology* **77**, 661–675. doi:10.1111/J.1095-8649.2010.02707.X

Carlson, J. K., Hale, L. F., Morgan, A., and Burgess, G. (2012). Relative abundance and size of coastal sharks derived from commercial shark longline catch and effort data. *Journal of Fish Biology* **80**, 1749–1764. doi:10.1111/J.1095-8649.2011.03193.X

Chabot, D., and Francis, C. M. (2016). Computer-automated bird detection and counts in high-resolution aerial images: a review. *Journal of Field Ornithology* **87**, 343–359. doi:10.1111/JOFO.12171

Chapman, B. K., and McPhee, D. (2016). Global shark attack hotspots: identifying underlying factors behind increased unprovoked shark bite incidence. *Ocean and Coastal Management* **133**, 72–84. doi:10.1016/J.OCECOAMAN.2016.09.010

Cliff, G., and Dudley, S. F. (2011). Reducing the environmental impact of shark-control programs: a case study from KwaZulu–Natal, South Africa. *Marine and Freshwater Research* **62**, 700–709. doi:10.1071/MF10182

Colefax, A. P., Butcher, P. A., and Kelaher, B. P. (2018). The potential for unmanned aerial vehicles (UAVs) to conduct marine fauna surveys in place of manned aircraft. *ICES Journal of Marine Science* **75**, 1–8. doi:10.1093/ICESJMS/FSX100

Colefax, A. P., Butcher, P. A., Pagendam, D. E., and Kelaher, B. P. (2019). Reliability of marine faunal detections in drone-based monitoring. *Ocean and Coastal Management* **174**, 108–115. doi:10.1016/J.OCECOAMAN.2019.03.008

de Freitas, C. R. (2015). Weather and place-based human behavior: recreational preferences and sensitivity. *International Journal of Biometeorology* **59**, 55–63. doi:10.1007/S00484-014-0824-6

Dewar, H., Domeier, M., and Nasby-Lucas, N. (2004). Insights into young of the year white shark, *Carcharodon carcharias*, behaviour in the Southern California Bight. *Environmental Biology of Fishes* **70**, 133–143. doi:10.1023/B:EBFI.0000029343.54027.6A

Dicken, M. L., and Booth, A. J. (2013). Surveys of white sharks (*Carcharodon carcharias*) off bathing beaches in Algoa Bay, South Africa. *Marine and Freshwater Research* **64**, 530–539. doi:10.1071/MF12336

Engelbrecht, T., Kock, A., Waries, S., and O'Riain, M. J. (2017). Shark spotters: successfully reducing spatial overlap between white sharks (*Carcharodon carcharias*) and recreational water users in False Bay,

South Africa. *PLoS One* **12**, e0185335. doi:10.1371/JOURNAL.PONE.0185335

Evans, L. J., Hefin Jones, T., Pang, K., Evans, M. N., Saimin, S., and Goossens, B. (2015). Using drone technology as a tool for behavioral research: a case study of crocodilian nesting. *Herpetological Conservation and Biology* **10**, 90–98.

Fiori, L., Doshi, A., Martinez, E., Orams, M. B., and Bollard-Breen, B. (2017). The use of unmanned aerial systems in marine mammal research. *Remote Sensing* **9**, 543. doi:10.3390/RS9060543

Fleming, P. J. S., and Tracey, J. P. (2008). Some human, aircraft and animal factors affecting aerial surveys: how to enumerate animals from the air. *Wildlife Research* **35**, 258–267. doi:10.1071/WR07081

Froeschke, J. T., Froeschke, B. F., and Stinson, C. M. (2013). Long-term trends of bull shark (*Carcharhinus leucas*) in estuarine waters of Texas, USA. *Canadian Journal of Fisheries and Aquatic Sciences* **70**, 13–21. doi:10.1139/CJFAS-2012-0037

Fuentes, M. M. P. B., Bell, I., Hagihara, R., Hamann, M., Hazel, J., Huth, A., Seminoff, J. A., Sobtzick, S., and Marsh, H. (2015). Improving in-water estimates of marine turtle abundance by adjusting aerial survey counts for perception and availability biases. *Journal of Experimental Marine Biology and Ecology* **471**, 77–83. doi:10.1016/J.JEMBE.2015.05.003

Gibbs, L., and Warren, A. (2015). Transforming shark hazard policy: learning from ocean-users and shark encounter in Western Australia. *Marine Policy* **58**, 116–124. doi:10.1016/J.MARPOL.2015.04.014

Gu, J., Wang, Z., Kuen, J., Ma, L., Shahroudy, A., Shuai, B., Liu, T., Wang, X., and Wang, G. (2018). Recent advances in convolutional neural networks. *Pattern Recognition* **77**, 354–377. doi:10.1016/J.PATCOG.2017.10.013

Hagihara, R., Jones, R. E., Grech, A., Lanyon, J. M., Sheppard, J. K., and Marsh, H. (2014). Improving population estimates by quantifying diving and surfacing patterns: a dugong example. *Marine Mammal Science* **30**, 348–366. doi:10.1111/MMS.12041

Hart, N. S., and Collin, S. P. (2015). Shark senses and shark repellents. *Integrative Zoology* **10**, 38–64. doi:10.1111/1749-4877.12095

Hazin, F. H. V., and Afonso, A. S. (2014). A green strategy for shark attack mitigation off Recife, Brazil. *Animal Conservation* **17**, 287–296. doi:10.1111/ACV.12096

Hazin, F. H. V., Burgess, G. H., and Carvalho, F. C. (2008). A shark attack outbreak off Recife, Pernambuco, Brazil: 1992–2006. *Bulletin of Marine Science* **82**, 199–212.

Hazin, F. H. V., Afonso, A. S., De Castilho, P. C., Ferreira, L. C., and Rocha, B. C. L. M. (2013). Regional movements of the tiger shark, *Galeocerdo cuvier*, off northeastern Brazil: inferences regarding shark attack hazard. *Annals of the Brazilian Academy of Sciences* **85**, 1053–1062. doi:10.1590/S0001-37652013005000055

Hodgson, A., Kelly, N., and Peel, D. (2013). Unmanned aerial vehicles (UAVs) for surveying marine fauna: a dugong case study. *PLoS One* **8**, e79556. doi:10.1371/JOURNAL.PONE.0079556

Holland, K. N., Wetherbee, B. M., Lowe, C. G., and Meyer, C. G. (1999). Movements of tiger sharks (*Galeocerdo cuvier*) in coastal Hawaiian waters. *Marine Biology* **134**, 665–673. doi:10.1007/S002270050582

Jones, G. P., Pearlstine, L. G., and Percival, H. F. (2006). An assessment of small unmanned aerial vehicles for wildlife research. *Wildlife Society Bulletin* **34**, 750–758. doi:10.2193/0091-7648(2006)34[750:AAOSUA]2.0.CO;2

Kelaher, B. P., Colefax, A. P., Tagliafico, A., Bishop, M. J., Giles, A., and Butcher, P. A. (2019). Assessing variation in assemblages of large marine fauna off ocean beaches using drones. *Marine and Freshwater Research*. doi:10.1071/MF18375

Kessel, S. T., Gruber, S. H., Gledhill, K. S., Bond, M. E., and Perkins, R. G. (2013). Aerial survey as a tool to estimate abundance and describe distribution of a carcharhinid species, the lemon shark, *Negaprion brevirostris*. *Journal of Marine Biology* **2013**, 1–10. doi:10.1155/2013/597383

Kiszka, J. J., Mourier, J., Gastrich, K., and Heithaus, M. R. (2016). Using unmanned aerial vehicles (UAVs) to investigate shark and ray densities in a shallow coral lagoon. *Marine Ecology Progress Series* **560**, 237–242. doi:10.3354/MEPS11945

Kleen, J. M., and Breland, A. D. (2014). Increases in seasonal manatee (*Trichechus manatus latirostris*) abundance within Citrus County, Florida. *Aquatic Mammals* **40**, 69–80. doi:10.1578/AM.40.1.2014.69

Koski, W. R., Allen, T., Ireland, D., Buck, G., Smith, P. R., Macrander, A. M., Halick, M. A., Rushing, C., Sliwa, D. J., and McDonald, T. L. (2009). Evaluation of an unmanned airborne system for monitoring marine mammals. *Aquatic Mammals* **35**, 347–357. doi:10.1578/AM.35.3.2009.347

Kudo, H., Koshino, Y., Eto, A., Ichimura, M., and Kaeriyama, M. (2012). Cost-effective accurate estimates of adult chum salmon, *Oncorhynchus keta*, abundance in a Japanese river using a radio-controlled helicopter. *Fisheries Research* **119–120**, 94–98. doi:10.1016/J.FISHRES.2011.12.010

Lemahieu, A., Blaison, A., Crochelet, E., Bertrand, G., Pennober, G., and Soria, M. (2017). Human–shark interactions: the case study of Reunion Island in the south-west Indian Ocean. *Ocean and Coastal Management* **136**, 73–82. doi:10.1016/J.OCECOAMAN.2016.11.020

Linchant, J., Lisein, J., Semeki, J., Lejeune, P., and Vermuelen, C. (2015). Are unmanned aircraft systems (UASs) the future of wildlife monitoring? A review of accomplishments and challenges. *Mammal Review* **45**, 239–252. doi:10.1111/MAM.12046

Martin, J., Edwards, H. H., Burgess, M. A., Percival, H. F., Fagan, D. E., Gardner, B. E., Ortega-Ortiz, J. G., Ifju, P. G., Evers, B. S., and Rambo, T. J. (2012). Estimating distribution of hidden objects with drones: from tennis balls to manatees. *PLoS One* **7**, e38882. doi:10.1371/JOURNAL.PONE.0038882

McAuley, R., Bruce, B., Keay, I., Mountford, S., and Pinnell, T. (2016). Evaluation of passive acoustic telemetry approaches for monitoring and mitigating shark hazards off the coast of Western Australia. Fisheries Research Report No. 273, Department of Fisheries, Western Australia, Perth.

McPhee, D. (2014). Unprovoked shark bites: are they becoming more prevalent? *Coastal Management* **42**, 478–492. doi:10.1080/08920753.2014.942046

McPhee, D., and Blount, C. (2015). Shark deterrents and detectors review of bather protection technologies. Report prepared for NSW Department of Primary Industries, Cardno, St Leonards, NSW.

Meeuwig, J. J., and Ferreira, L. C. (2014). Moving beyond lethal programs for shark hazard mitigation. *Animal Conservation* **17**(4), 297–298. doi:10.1111/ACV.12154

Neff, C. (2012). Australian beach safety and the politics of shark attacks. *Coastal Management* **40**, 88–106. doi:10.1080/08920753.2011.639867

Neff, C., and Heuter, R. (2013). Science, policy, and the public discourse of shark "attack": a proposal for reclassifying human–shark interactions. *Journal of Environmental Studies and Sciences* **3**, 65–73. doi:10.1007/S13412-013-0107-2

O'Connell, C. P., Abel, D. C., Stroud, E. M., and Rice, P. H. (2011). Analysis of permanent magnets as elasmobranch bycatch reduction devices in hook-and-line and longline trials. *Fishery Bulletin* **109**, 394–401.

O'Connell, C. P., Hyun, S.-Y., Gruber, S. H., O'Connell, T. J., Johnson, G., Grudecki, K., and He, P. (2014*a*). The use of permanent magnets to reduce elasmobranch encounter with a simulated beach net. 1. The bull shark (*Carcharhinus leucas*). *Ocean and Coastal Management* **97**, 12–19. doi:10.1016/J.OCECOAMAN.2013.12.012

O'Connell, C. P., Andreotti, S., Rutzen, M., Meÿer, M., and He, P. (2014*b*). The use of permanent magnets to reduce elasmobranch encounter with a simulated beach net. 2. The great white shark (*Carcharodon carcharias*). *Ocean and Coastal Management* **97**, 20–28. doi:10.1016/J.OCECOAMAN.2012.11.006

O'Connell, C. P., Stroud, E. M., and He, P. (2014*c*). The emerging field of electrosensory and semiochemical shark repellents: mechanisms of detection, overview of past studies, and future directions. *Ocean and Coastal Management* **97**, 2–11. doi:10.1016/J.OCECOAMAN.2012.11.005

O'Connell, C. P., Andreotti, S., Rutzen, M., Meÿer, M., and Matthee, C. A. (2018). Testing the exclusion capabilities and durability of the Sharksafe barrier to determine its viability as an eco-friendly alternative to current shark culling methodologies. *Aquatic Conservation* **28**(1), 252–258. doi:10.1002/AQC.2803

O'Donoghue, S. H., Drapeau, L., and Peddemors, V. M. (2010). Broad-scale distribution patterns of sardine and their predators in relation to remotely sensed environmental conditions during the KwaZulu–Natal sardine run. *African Journal of Marine Science* **32**(2), 279–291. doi:10.2989/1814232X.2010.501584

Parsons, M. J. G., Parnum, I. M., Allen, K., McCauley, R. D., and Erbe, C. (2015). Detection of sharks with the Gemini imaging sonar. *Acoustics Australia* **42**, 185–189.

Pepin-Neff, C., and Wynter, T. (2017). Shark bites and shark conservation: an analysis of human attitudes following shark bite incidents in two locations in Australia. *Conservation Letters* 1–8.

Pollock, K. H., Marsh, H. D., Lawler, I. R., and Aldredge, M. W. (2006). Estimating animal abundance in heterogeneous environments: an application to aerial surveys for dugongs. *The Journal of Wildlife Management* **70**, 255–262. doi:10.2193/0022-541X(2006)70[255:EAAIHE]2.0.CO;2

Poole, K. G., Cuyler, C., and Nymand, J. (2013). Evaluation of caribou *Rangifer tarandus groenlandicus* survey methodology in West Greenland. *Wildlife Biology* **19**, 225–239. doi:10.2981/12-004

R Development Core Team (2015). R: A Language and Environment for Statistical Computing. R Foundation for Statistical Computing, Vienna, Austria. Available at http://www.r-project.org [verified 1 December 2018].

Reid, D. D., Robbins, W. D., and Peddemors, V. M. (2011). Decadal trends in shark catches and effort from the New South Wales, Australia, Shark Meshing Program 1950–2010. *Marine and Freshwater Research* **62**, 676–693. doi:10.1071/MF10162

Ricci, J. A., Vargas, C. R., Singhal, D., and Lee, B. T. (2016). Shark attack-related injuries: epidemiology and implications for plastic surgeons. *Journal of Plastic, Reconstructive & Aesthetic Surgery* **69**, 108–114. doi:10.1016/J.BJPS.2015.08.029

Robbins, W. D., Peddemors, V. M., Kennelly, S. J., and Ives, M. C. (2014). Experimental evaluation of shark detection rates by aerial observers. *PLoS One* **9**, e83456. doi:10.1371/JOURNAL.PONE.0083456

Rowat, D., Gore, M., Meekan, M. G., Lawler, I. R., and Bradshaw, C. J. A. (2009). Aerial survey as a tool to estimate whale shark abundance trends. *Journal of Experimental Marine Biology and Ecology* **368**, 1–8. doi:10.1016/J.JEMBE.2008.09.001

Saqib, M., Daud Khan, S., Sharma, N., Scully-Power, P., Butcher, P., Colefax, A., and Blumenstein, M. (2018). Real-time drone surveillance and population estimation of marine animals from aerial imagery. In 'International Conference on Image and Vision Computing New Zealand', 19–21 November 2018, Auckland, New Zealand. pp. 1–6. (IEEE: Piscataway, NJ.)

Schoonmaker, J. S., Podobna, Y., and Boucher, C. D. (2011). Electro-optical approach for airborne marine mammal surveys and density estimations. *U.S. Navy Journal of Underwater Acoustics* **61**, 968–985.

Seymour, A. C., Dale, J., Hammill, M., Halpin, P. N., and Johnston, D. W. (2017). Automated detection and enumeration of marine wildlife using unmanned aircraft systems (UAS) and thermal imagery. *Scientific Reports* **7**, 45127. doi:10.1038/SREP45127

Smith, A. B, and Cullis, B. R. (2019). Design Tableau: an aid to specifying the Linear Mixed Model for a comparative experiment. Working Paper 5-18, NIASRA Working Paper Series. (University of Wollongong: Wollongong, Australia.) Available at https://niasra.uow.edu.au/content/groups/public/@web/@inf/@math/documents/mm/uow248255.pdf [verified 29 October 2019].

Stein, D., Stewart, S., Gilbert, G., and Schoonmaker, J. (1999). Band selection for viewing underwater objects using hyperspectral sensors. In 'SPIE Conference on Airborne and In-Water Underwater Imaging', 21–22 July 1999, Denver, CO, USA. Vol. 3761. pp. 50–61. (The International Society for Optical Engineering (SPIE): Bellingham, WA.)

Strobel, B., and Butler, M. (2014). Monitoring whooping crane abundance using aerial surveys: influences on detectability. *Wildlife Society Bulletin* **38**, 188–195. doi:10.1002/WSB.374

Sumpton, W. D., Taylor, S. M., Gribble, N. A., McPherson, G., and Ham, T. (2011). Gear selectivity of large-mesh nets and drumlines used to catch sharks in the Queensland Shark Control Program. *African Journal of Marine Science* **33**, 37–43. doi:10.2989/1814232X.2011.572335

West, J. G. (2011). Changing patterns of shark attacks in Australian waters. *Marine and Freshwater Research* **62**, 744–754. doi:10.1071/MF10181

Zhang, X., He, S., Shabani, A., Zhai, P. W., and Du, K. (2017). Spectral sea surface reflectance of skylight. *Optics Express* **25**, A1–A13. doi:10.1364/OE.25.0000A1